7 DIRECT SIMULATION MONTE-CARLO (DSMC) METHOD

7.1 INTRODUCTION

The *direct simulation Monte-Carlo* (*DSMC*) method [1, 2] developed by G. A. Bird is a method basing directly on the physical simulation of the gas flows. Concerning its relation with the Boltzmann equation there are references [3, 4, 5] and others proving its consistence with the Boltzmann equation. In fact, both DSMC method and the Boltzmann equation are based on the same physical reasoning. In handling the molecular collisions and the molecule surface interactions both methods need to introduce physical models. But as DSMC method deals with the actions of individual molecules, it is easier for it to introduce models in agreement with the physical realities, but it is relative difficult to involve the realistic models in the mathematical solution of the Boltzmann equation. This is all the more so in treating problems of gas flows accompanied by chemical reactions and radiation. And as the DSMC method does not depend on the assumption of inverse collisions, it can be applied to such complex phenomena as the recombination reactions involving three-body collisions, which is beyond the capability of the Boltzmann equation. Thus, it is unnecessary and impossible to verify each simulation procedure involving complicated physic-chemical processes by strict proof that it is derived from the Boltzman equation. But still the DSMC method is not a method independent of the Boltzmann equation or a method which stands side by side with the Boltzmann equation. The Boltzmann equation plays fundamental roles in the formulation of the DSMC method. For example, the various molecular models are based on the relation of the collision cross section with the gas viscosity given by the Chapman-Enskog approximation in the solution of the Boltzmann equation (see section 2.4). The sampling of collision pairs and the implementation of collisions in DSMC is based on ensuring the matching of motion and collisions

in simulation, keeping it consistent with the actual flow. This is achieved by the satisfaction of conditions expressed through collision cross sections depending in turn on the molecular models (see the explanation in section 7.2). On the other hand, the experimental verification played an important role for the general acceptance of the DSMC method. Both in the aspect of the global characteristics of the flow field and in the aspect of the micro-structure of the flow the DSMC method gave results in good agreement with the experimental data. The result of simulation by the DSMC obtained for the space shuttle in the transitional regime (including the ratio of drag to lift) [6] has excellent agreement with the flight experimental data. The experimental measurement of the distribution functions for the molecular velocity in the flow direction and for the velocity in the transverse direction in the strong shock wave structure was carried out as early as in 1966, but as the result obtained had poor agreement with the available at that time theoretical result (the Mott-Smith solution [7], see also section 6.3), so it had not been published until 1989, and was published in Science [8] only when the DSMC calculations were carried out and excellent agreement with the experimental result was obtained (see Fig. 7.1) and received general recognition of the scientific community. The verification of the DSMC method by the experiments enhanced its status and significance.

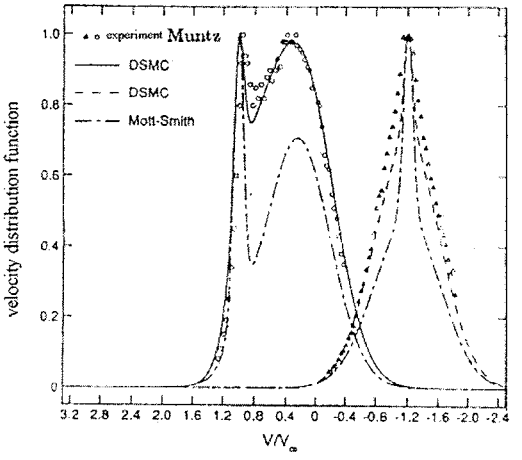

Fig. 7.1 The distribution functions of the parallel and normal velocities in the structure of normal shock wave of helium ($Ma = 25$ at $\bar{x} = 0.565$), comparison of the DSMC calculation and the experimental measurements [8]

The DSMC method employs a large number of simulated molecules to simulate the real gas. The number of simulated molecules must be large enough so that in the cells of the flow field they can fully represent the distribution of the real gas molecules. At the same time this number is much smaller than the number of real molecules, i.e., each simulated molecule represents an enormous number of real molecules. In the computer the position coordinates, the velocity components and the internal energies of each simulated molecules are stored, they are changing with the motion of molecules, their encounters with the boundaries and the collisions between themselves unceasingly. The time parameter in the simulation is identical with the physical time in the real flow. All computations are unsteady, the steady flow is obtained as the long time asymptotic state of the unsteady flow. The essential approximation of the DSMC method is: in a small time step Δt the molecular motion is decoupled with the molecular collisions. In time Δt each simulated molecule moves a certain distance according to its velocity, then the representative collisions between the molecules in time Δt are calculated. The time step Δt must be small in comparison with the local mean collision time. The flow filed is divided into cells of linear size Δr used to choose collision pairs among molecules in them, and also to sum molecular quantities to obtain the macroscopic characteristics of the flow field. The size of Δr should be small in comparison with the scale length of the gradient of the macroscopic quantities of the flow field, in general, letting Δr to be 1/3 or so of the mean free path can satisfy this condition. Corresponding to the motion in time Δt, how to choose the collision pairs and how many representative collisions are to be implemented, is a key issue in ensuring the consistency of the simulation with the processes occurred in real gas. This issue will be discussed specially in the next section.

The calculation of the motion in time Δt is a simple and direct deterministic step. Whenever a molecule encounters with the boundary the interaction of it with the boundary is taken into account, the DSMC method allows the introduction of various reflection models, about them detailed discussion has been given in Chapter 3. Except the specular reflection, which is a simple deterministic action, the implementation of the diffuse reflection, the Maxwellian reflection and the CLL model reflection requires the employment of the random fraction in obtaining the sampling of the velocity after reflection (see sections 3.2 and 3.4). Then the

molecules move according to the after-collision velocities, and the new positions the molecules move to in the remaining time are obtained.

What are the velocities of the molecules after collisions depends on what kind of molecular models are being employed, this plays a determinant role in the exact modeling of the real gas flows. The DSMC method allows the introduction of the phenomenological models capable of reflecting the essential features of the flow field, in particular, the VHS model, the VSS model, the GHS model and the GSS model and their implementation in the DSMC simulations have been discussed in sections 2.4.4~2.4.7.

In section 7.2 the sampling and the counting of collisions will be discussed, in section 7.3 the implementation of the DSMC method will be explained through a simple example of Couette flow. In sections 7.4 and 7.5 the methods of handling the excitation and relaxation of the internal energies and the chemical reactions are introduced. In section 7.6 some development of the general codes in solving the complicated flow field and the position element method are introduced.

7.2 SAMPLING OF COLLISIONS

The essential idea of the DSMC method is the decoupling of the molecular motion and collisions. The correct implementation of the collision sampling, i.e., the appropriate choice of the collision pairs and the implementation of a certain number of collisions is the key issue in ensuring the matching of the collisions with motion in time Δt and the consistency of the simulation with the actual flow processes.

The way of implementation by the *time counter* (*TC*) method introduced by Bird [1] is: (1) Choose one pair randomly from all available molecules out of a cell; (2) Take

$$S(c_r)/S_{\max}, \tag{7.1}$$

as criterion, where $S(c_r)=c_r\sigma_T$, $S_{\max}$ is the maximum of $S(c_r)$ in the cell. To this apply the acceptance-rejection method to determine if this pair is selected, if not, return to (1); (3) If the pair is selected the collision is calculated according to the molecular model, the cell time is advanced a value

$$\Delta t_c = \left[\frac{nN}{2} S(c_r)\right]^{-1}, \tag{7.2}$$

where n and N are the number density and the number of molecules in the cell; (4) the processes (1), (2), (3) are repeated until the cell time exceeds Δt.

The mean collision frequency of the molecules is (see Eq. (2.207))

$$\nu = n\overline{S(c_r)}. \tag{7.3}$$

The number N_t of collisions occurred in time Δt within a cell is

$$N_t = \frac{N}{2}\nu\Delta t = \frac{nN}{2}\overline{S(c_r)}\Delta t. \tag{7.4}$$

From Eq. (7.4) it is seen intuitively, that whenever a collision occurs, letting the cell time to advance a value Δt_c (see Eq. (7.2)) will ensure the correct collision frequency in the cell. There is a strict analytic proof in reference [1].

The TC method had been widely used for its high efficiency and for it can ensure the correct collision frequency when the number of molecules in a cell is large enough. But when the number of molecules in a cell is not large enough, the occasionally selected collision with very small probability ($S(c_r)/S_{\max}$ very small) would make the cell time advance too long a time (surpassing several Δt) and distort the collision frequency, leading to errors. Koura [9] suggested the *nil collision* (*NL*) method, Ivanov et al. [10] suggested the *major frequency* (*MF*) method, which can overcome this defect of the TC method and does not lead to much increase of the computation time.

Bird [11] suggested the *no time counter* (*NTC*) method, which is widely used in many simulations. The NTC method is a modification of the *direct* or *Kac method*. The direct method considers all possible collision pairs in a cell, the number of them is

$$N_D = \frac{N(N-1)}{2}. \tag{7.5}$$

The probability P_D of the occurrence of collision of the two molecules of one collision pair in time Δt equals to the ratio of the volume swept by the collision section with the relative velocity c_r to the cell volume

$$P_D = \frac{F_N S \Delta t}{V_c}, \tag{7.6}$$

where F_N is the number of the actual molecules one simulated molecule represents. The efficiency of the direct method is low, for P_D is very small, and the computation time needed for all collision pairs is proportional to the squire of the number N of molecules in the cell. The NTC method only considers a very small portion of the N_D collision pairs (N_D is multiplied by a small factor), but at the same time P_D is amplified accordingly by the reciprocal of the same proportionality. It is readily seen that when this small factor is taken as

$$F_N S_{\max} \Delta t / V_c ,$$

the probability of occurrence of the collision is changed into

$$P_{NTC} = S / S_{\max} ,$$

that is , is equal to the criterion Eq. (7.1) of TC method. And, the number of the collision pairs need to be considered is changed accordingly

$$N_{NTC} = \frac{N\overline{N}}{2} F_N S_{\max} \Delta t / V_c , \tag{7.7}$$

where as F_N is large, $N(N-1)/2$ was replaced by $N^2/2$, and to keep the linear relation of N_{NTC} with the random number N , N^2 was replaced by $N\overline{N}$ ($\overline{N}$ is the time or ensemble average of N). Noting that $\overline{N}F_N/V_c$ in fact is the number density n in the flow field, then according to Eq. (7.7) the number of collision pairs to be considered is actually

$$N_{NTC} = \frac{nN}{2} S_{\max} \Delta t . \tag{7.8}$$

The probability that the collision pair is selected is given by Eq. (7.1), it is seen that the number of collisions that actually happened agrees with the theoretical value (Eq. (7.4)).

We suggested the *randomly sampled frequency* (*RSF*) method [12]. The way of implementation of it is: M pairs of molecules are randomly selected from all possible pairs with returning back when not selected, take

$$\overline{S}_{RSF} = \frac{1}{M}\sum_{j=1}^{M} S(c_{rj}) \tag{7.9}$$

as the estimate of $\overline{S(c_r)}$, thus the number of collisions occurred in each cell is (see Eq. (7.4))

$$N_{RSF} = \frac{nN}{2}\overline{S}_{RSF}\Delta t\,. \tag{7.10}$$

The pairs of molecules are chosen following the same steps as in the TC method and are accepted or rejected until the number of collisions reaches the number of Eq. (7.10). The analysis and test calculation in [12] show that, when M is chosen as 1, sufficient accuracy can be reached.

Note, the NTC method calculates the number of collisions pairs that need to be considered according to Eq. (7.8), while the RSF method calculates the number of collisions that should happen in each cell according to Eq. (7.10), all these numbers thus calculated have to be rounded-off to integers and the remainders of the number of collisions have to be stored. The concrete way of doing will be elucidated in the practical example.

7.3 EXAMPLE OF SOLUTION OF PROBLEM BY THE DSMC METHOD

In this section the details of concrete implementation of the DSMC method is presented through the example of a simple, one-dimensional problem of *Couette flow*. The space between two parallel plane plates separated by a distance $Y-LENGTH=\lambda/Kn$ is filled with gas of temperature $273K$ and pressure $0.01atm$. The lower plate is located at $y=0$ and moves with a velocity $U\_WALL/2$ in the direction of positive x, the upper plate is located at $y=Y-LENGTH$ and moves with a velocity $-U\_WALL/2$ in the direction of negative x. The wall temperatures of the two plates are the same as the gas tem-

perature, the gas molecules are reflecting diffusely at the wall. The FORTRAN program of the solution of the Couette flow problem is listed in APPENDIX IV.

The flow chart of the program of problem by the DSMC method is shown in Fig.7.2. This flow chart is suitable for the solution of any flow problem, and includes the cases of steady and unsteady flows. The program of the present example also follows this chart. The FORTRAN code of the Couette flow problem consists of the main program, the FUNCTION RF(IDUM) generating the random fraction and 7 subroutines. The 7 subroutines correspond to the 7 steps in the flow chart (see Fig 7.2):

subc1 set constants and initial values

subc2 set the initial velocities and positions of molecules

subc3 calculation of the motion and the reflection of the simulated molecules at the surfaces

subc4 the reordering and the indexing of the molecules

subc5 calculation of the collisions

subc6 sampling of the flow properties

subc7 the summation of the characteristics of the flow field and on the surfaces

In the main program first the adjustable number of cells (no-cell), the number of molecules in each cell (no-molecule-each-cell) and the total number of molecules (no-molecule) are specified by the PARAMETER statement. As the IP (information preservation) method introduced in the next Chapter uses the same program for illustration, the statements needed for the IP method are marked by the symbols * and **. The former marks statement that is used to replace the one before it, the latter marks the statement that needed to be added anew. For example, the IP method needs to use different number of cells (no-cell, 300 is used to replace 50) and different total number of molecules (no-molecule, 9000 to replace 1500), so the PARAMETER statements marked by * are used to specify the values required by the IP method. Then the COMMON and DIMENSION statements introduce the variables which are commented in detail in the program and are not explained here. After the assignment of the reverse *rkn* of the *Kn* number, i.e., the specification of the *Kn* number, the subroutines of subc1,... are called successively to implement the various steps of the DSMC simulation. Note

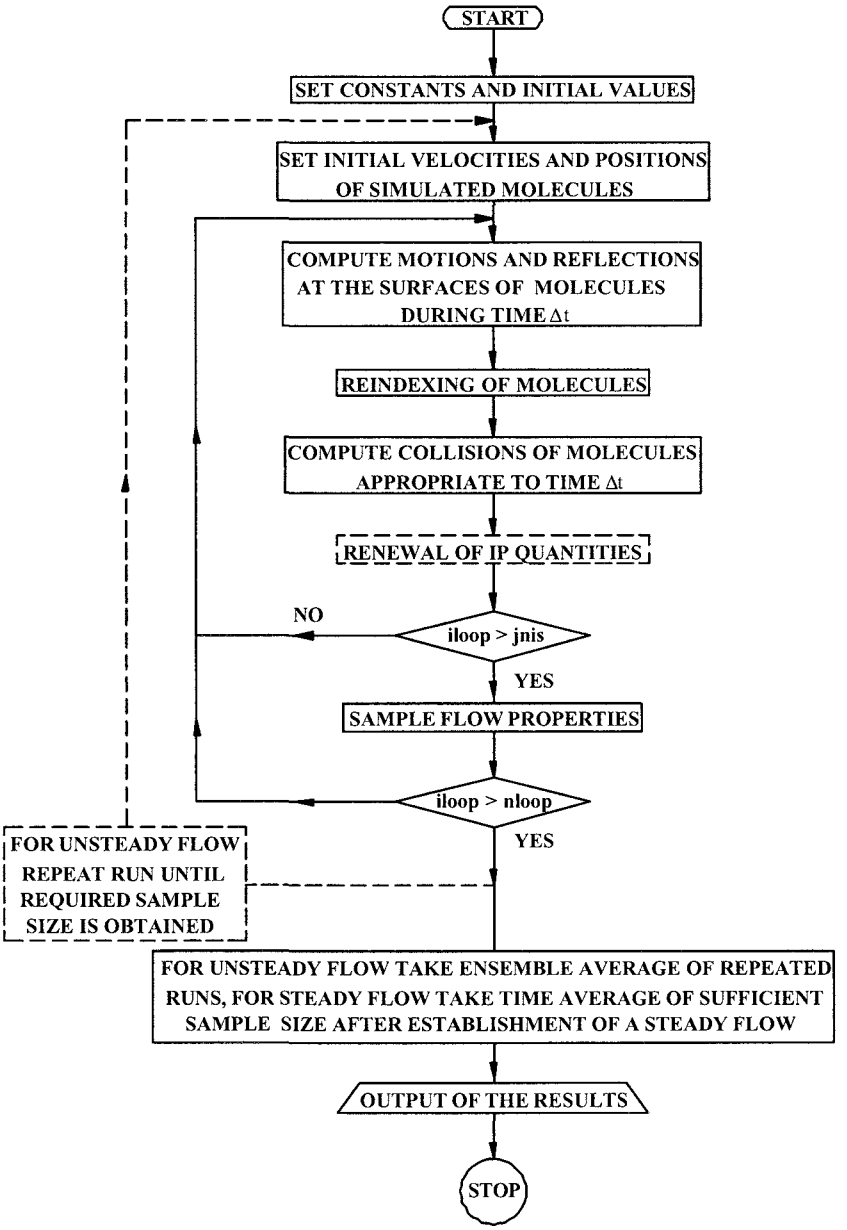

Fig. 7.2 Flow chart of program of the DSMC-IP method

in the program the following parameters are used to judge whether the code continues to proceed or goes back to the beginning of a loop.

iloop: the number of current loops; *jnis*: the number of loops at which the sampling starts; *nloop*: the total number of loops.

The statement CONTINUE labeled 100 is the position where the loop starts, after it the loop counter *iloop* adds 1 to the record. After the calculation of collisions by calling subc5 judge if the number (*iloop*) of current loops is larger than the number (*jnis*) of loops at which the sampling starts. If yes, the quantities on the wall and in the flow field are sampled, if no, provided that *iloop* is less than *nloop* go back to the beginning of the loop labeled 100. Proceed the cycle until the total number (*nloop*) of loops is reached, and then accomplish the sampling and output. The surface parameters are stored in surf-cout.dat and the flow field parameters are stored in u-cou.dat.

In the subroutine **subc1** SET CONSTANTS AND INITIAL VALUES, the ordinary constants are exp lained by the comment lines following them. As helium is chosen as the media and HS model is adopted DIAREF is taken as $3.659\times10^{-10}m$ (Table 2 of Appendix I). In the IP method DIAREF is taken as $3.963\times10^{-10}m$, this statement is marked with $*$. Although in the present program the HS model is adopted, but in preparing the expression for TKOM to be used in the calculation of the collision frequency the notation of VHS-coe is retained, all one has to do is let $VHS-coe=(\Gamma(5/2-\omega))^2$, the VHS model is obtained (see the comment line before the assignment statement of TKOM). Then the initial temperature, pressure and the number density FND are set. Note, that in the DSMC method the wall velocity U-WALL is taken as $100m/s$, but in the IP method the wall velocity U-WALL is taken as $1.0m/s$. The molecular mean free path λ (AMDA) is calculated according to the hard sphere model (see Eq. (2.221)). The scope of the flow field Y-LENGTH is taken as λ/Kn, and the time step DTM is taken as $0.23\lambda/c_m$, where c_m is the initial most probable speed denoted by VM_INI in the program. AREA is a representative cross section area through which we observe the flow field corresponding to the number of molecules and normal to the direction (y direction) of variation of the flow field. In the whole flow field only NO-MOLECULE molecules are introduced, and the scope of the flow field in the y direction is Y-LENGTH. If we observe the NO-MOLECULE molecules through

AREA obtained in the program, then the number density in the simulation is just the initial number density FND (=NO_MOLECULE/Y_LENGTH * AREA). This AREA will be needed when calculating the molecular flux towards the surface.

In the subroutine **subc2** the initial velocities and positions of all simulated molecules are given. The initial velocity is the initial macroscopic velocity plus the thermal velocity in the equilibrium gas, the generation of the components of the latter see Eq. (3.18) and Eq. (3.19) and the discussion followed in section 3.2. In the allocation of the positions of the simulated molecules in the cells first the molecules are distributed according to the number NO_MOLECULE _EACH_CELL of molecules in each cell to various cells, and then assign randomly the locations of the NO_MOLECULE molecules in various cells. In comparison with the direct allocation of all the simulated molecules between 0 and Y_LENGTH this method has taken into account the variance reduction principle. In fact, according to Eq. (III.5) of the Appendix, in which if take $b = Y\_LENGTH, a = 0$, x would be the random position of the molecule, but the scatter-deviation would be very large. Following the variance reduction principle the sampling should have been taken according to (III.5)', and should take $m =$ NO_MOLECULE, the positions of the molecules of the initial distribution possesses the reduced variance. It is a general issue to take into account the variance reduction principle, for example, when allocate the initial positions of the oncoming molecules in three-dimensional flows, the equation (III.5)' should be repeatedly used in two directions normal to the oncoming flow to fix the initial coordinates of the molecules.

The subroutine **subc3** is used to calculate the motion of molecules and the reflection and sampling at the upper and lower plates. Detailed explanation is given in the comment lines of the program for the upper plate. Note, before the accumulative counting of the contribution of the incident molecules, the reference frame is transferred to be connected with the upper plate (moving with velocity –U_WALL/2). In the DSMC method it is required that $p(1,m) = p(1,m) + U\_WALL/2.d0$, for the IP method it is required that $vmean(1,m) = vmean(1,m) + U\_WALL/2.d0$. In UP_WALL(I), I=1, 2, 3, 4, the following quantities of the incident molecules are accumulatively counted: (1) number of molecules; (2) tangential momentum; (3) normal momentum; (4) kinetic energy. For

the sampling of the molecular velocities after the diffuse reflection from the plate see Eqs. (3.18), (3.19), (3.15) and (3.20) of section 3.2. In UP_WALL(I), I=5, 6, 7 the following quantities of the reflected molecules are accumulatively counted: (5) tangential momentum; (6) normal momentum; (7) kinetic energy. Then the reference frame is transferred back to be connected with the stationary system and the new positions the molecules move to are calculated. The reflection and the sampling on the lower plate are similar with those on the upper plate.

The subroutine **subc4** is used for the reordering and indexing of the molecules. The molecule with the original identifying number M moves into the cell with order number NCELL. IC(1,I) stores the number of molecules in the Ith cell, IC(2,I) stores the order number of the first molecule in the Ith cell minus 1. When recounting IC(1,NCELL), by letting $K = IC(2, NCELL) + IC(1, NCELL)$ the new order number K of the molecule with the original identifying number M is obtained. The original number M is stored in LCR(K).

The subroutine **subc5** is used to calculate the collisions. Subroutine consists of a loop which successively calculates collisions in each cell. Before the label 300 the average (TKOM * VAVER) of $S(c_r)$ (see Eq. (7.1) and below) in the cell is calculated, and the number of collisions N_{RSF} (CNOIC, see Eq. (7.10)) that should occur in the cell according to the randomly sampled frequency method is obtained. Take into account the stored remainder of the number of collisions and after rounding-off anew the number of collisions NCOLL that should actually happen is calculated. After the label 300 two molecules are chosen randomly from the cell and are been examined whether they are selected or not according to the step involving Eq. (7.1), if yes, the velocities after collision are calculated, this process continues until the number of collisions in the cell reaches NCOLL, and the collisions in the next cell are calculated. In the above the number of collisions in a cell is controlled by the randomly sampled frequency method. The NTC method is the most used method for controlling the number of collisions. It is readily to modify the present program to shift to the NTC method. For this one needs to calculate first, before the label 300, the number N_{NTC} of collision pairs to be considered in the cell (see Eq. (7.8)), where $S_{\max}$ is obtained by multiplying TKOM by YRMAN_ETA51, and then change the program segment between the statement labeled 300 and the statement labeled 140 into a program segment cy-

cling N_{NTC} times (the number N_{NTC} obtained from Eq. (7.8) should be rounded-off and the remainder of the number of collisions should be stored, etc.).

The subroutine **subc6** runs the summation of the parameters of the flow field and stores the results in FIELD(N, NO_CELL), the subroutine **subc7** outputs these parameters and stores the parameters on the surface in surf-coue.dat, the parameters of the flow field in u_coue.dat.

The program of the present section has been aimed at the problem of Couette flow, but is readily modified to be applied to the solution of the problem of the Poiseuille flow and the Rayleigh probem. *Poiseuille flow* as the Couette flow is a steady flow problem, so the structure of the main program is not changed, the changes are limited to the changes in subroutine subc 3. At the plate surfaces the condition of stationary wall is put forward. At the same time, due to the influence of the pressure gradient the velocities of the molecules during every time DTM gain increments, which can be found from the momentum conservation equation. When the change of the pressure is given by the following equation

$$p = p_0\left(1+\alpha x/h\right),$$

where $h = Y\_LENGTH$ is the distance between the two plates, the increment of the velocity in Δt can be found to be (cf. the beginning part of section 8.5)

$$\Delta u = -\left(\alpha p_0/\rho h\right)\Delta t\,. \tag{7.11}$$

This increment is to be added to the thermal velocities and the IP velocities of the simulated molecules. The molecules are retarded near the plate surfaces. The equilibrium between acceleration and the retardation enable the flow to reach the steady state.

For the *Rayleigh problem* according to its geometric condition the boundary conditions in the subroutine subc3 is certainly to be modified. The lower plate moves with velocity U_WALL in the positive direction of x. The scope of the flow field Y_LENGTH should be taken large enough, so that the disturbance originated from the lower plate could not reach the upper boundary of the flow field during the time interval we are interested in. At the same time the specular

reflection boundary condition is set at the upper plane of the boundary. As the Rayeigh problem is an unsteady flow problem, so the structure of the main program must be changed. The location of the beginning of the loop, i.e., the location of the CONTINUE statement labeled 100 and the statement $illop = illop + 1$ following it, should be shifted from the location before CALL SUBC3 to that before CALL SUBC 2 (set the initial velocities and positions of the molecules). The conditional statement after CALL SUBC5 is to be cancelled, the program segment between CALL SUBC 3 and CALL SUBC 6 is to be made a loop by a DO statement to accomplish repeatedly the procedures "calculation of the molecular movement", "the indexing of the molecules", "the calculation of collisions" and "the sampling of flow properties", thus obtain the parameters of the flow field and on the surface at various time moments. The conditional statement after the loop is to allow return to the statement with label 100, so that to start the loop beginning from the initial state. This is to ensure the obtaining of large enough sampling size at various time moments utilizing the ensemble averaging, this is necessary for small storage of the micro computers. If the workstation of large enough storage is available, it is not necessary to restart the whole process from the statement labeled 100, obtaining large enough sampling size with one run is possible. This is the right means to demonstrate an unsteady process in real-time and to study the problem of instability.

7.4 THE EXCITATION AND RELAXATION OF THE INTERNAL ENERGIES

7.4.1 INTRODUCTION OF PHENOMENALOGICAL MODELS

For diatomic and polyatomic molecules, as we have seen in Chapter 1, the molecules possess as well internal energies, i.e., the rotational and vibrational energies. How to simulate the behavior of the internal energies in the direct simulation is the issue to be resolved in this section. In the equilibrium state various molecules can be assigned according to Eq. (1.94) certain rotational energy ($\zeta = 2$) and vibrational energy (ζ_v given by Eq. (1.86)). The problem of how to simulate the energy exchange between molecules in the collision is to be solved. Introduction of

the traditional models that reflect the diatomic characteristics of the molecules, such as the model of dual repulsive centers, the sphero-cylindrical model, the rough-sphere model and the harmonic oscillator model, into the DSMC simulation is unpractical, for in the simulation an enormous number of collisions must be computed. And for the purpose of simulation it is essential to know, how the energies are distributed after the collisions, and to ensure, that the rate of excitation and relaxation of the internal energies be in agreement with that given by the experiments. Larsen and Borgnakke [13, 14] introduced a phenomenological model and resolved this problem. The central idea is to assume that the kinetic energy (expressed by the relative velocities) and the internal energy follow the conservation of energies, the internal energy after collision is sampled according to the equilibrium distribution of the combination of the kinetic energy and the internal energy, and the rate of relaxation process of the energy is determined by adjusting the proportion of the elastic collisions and the inelastic collisions to make it satisfy the result obtained from the experiment. Such an approach is very simple in the conceptual and implemental aspects, and needs not much computation time. Such phenomenological philosophy deserves attention in approaching other problems. In the following the Larsen-Borgnnake model will be described, firstly in the assumption of the continuum distribution of the internal energies, the case of collision between molecules of different components in a gas mixture will be discussed. When discussing the continuum distribution of the vibrational energy, the combined cumulative distribution acceptance-rejection method in handling the distributions with singularities own to $\zeta_v < 2$ is introduced. Then the implementation of the Larsen-Borgnakke model in the case of discrete vibrational energy levels is discussed. Finally, the adjustment of the relaxation time by introducing the exchange probability of the vibrational energy is discussed.

7.4.2 IMPLEMENTATION OF LARSEN-BORGNAKKE MODEL

In this section the Larsen-Borgnakke model is explained on the example of collision between molecules of different components in the gas mixture. According to Eq. (1.94) the distribution functions of internal energies of component 1 and component 2 are proportional to

$$f(\varepsilon_{i1}) \propto \varepsilon_{i1}^{\frac{\zeta_1}{2}-1} e^{-\frac{\varepsilon_{i1}}{kT}}, \tag{7.12}$$

$$f(\varepsilon_{i2}) \propto \varepsilon_{i2}^{\frac{\zeta_2}{2}-1} e^{-\frac{\varepsilon_{i2}}{kT}}, \tag{7.13}$$

respectively. Now the distribution function of the total energy of the collision pair

$$E_i = \varepsilon_{i1} + \varepsilon_{i2} \tag{7.14}$$

is to be found according to Eq. (7.12) and (7.13).

The probability that the internal energy of component 1 is in the interval from $\varepsilon_{i,1}$ to $\varepsilon_{i,1} + d\varepsilon_{i,1}$ and the internal energy of component 2 is in the interval from $\varepsilon_{i,2}$ to $\varepsilon_{i,2} + d\varepsilon_{i,2}$ is proportional to

$$\varepsilon_{i,1}^{\frac{\zeta_1}{2}-1} \left(E_i - \varepsilon_{i,1}\right)^{\frac{\zeta_2}{2}-1} e^{-\frac{E}{kT}} d\varepsilon_{i,1} d\varepsilon_{i,2}. \tag{7.15}$$

Fix first the value of $\varepsilon_{i,1}$, then $dE_i = d\varepsilon_{i,2}$, the integration over $\varepsilon_{i,1}$ from 0 to E_i results in that the probability that the total internal energy is in the interval from E_i to $E_i + dE_i$ is proportional to

$$f(E_i)\,dE_i \propto \left(\int_0^{E_i} \varepsilon_{i,1}^{\frac{\zeta_1}{2}-1} \left(E_i - \varepsilon_{i,1}\right)^{\frac{\zeta_2}{2}-1} d\varepsilon_{i,1} \right) \cdot e^{-\frac{E_i}{kT}} dE_i =$$

$$E_i^{\frac{\zeta_1+\zeta_2}{2}-1} \frac{\Gamma\left(\frac{\zeta_1}{2}\right)\Gamma\left(\frac{\zeta_2}{2}\right)}{\Gamma\left(\frac{\zeta_1+\zeta_2}{2}\right)} e^{-\frac{E_i}{kT}} dE_i,$$

that is

$$f(E_i) \propto E_i^{\frac{\zeta}{2}-1} \exp\left[-\frac{E_i}{kT}\right], \tag{7.16}$$

where

$$\overline{\zeta} = \frac{\zeta_1 + \zeta_2}{2} \tag{7.17}$$

is the mean value of the internal degrees of freedom of the two molecules.

In section 2.11 we discussed the mean value of the quantity Q in collision and obtained the expression Eq. (2.224). Expressing the relative velocity c_r by the relative translational energy $\varepsilon_t = (1/2)m_r c_r^2$, one obtains

$$\overline{Q} \propto \int_0^\infty Q \varepsilon_t^{3/2-\omega} \exp\left(-\frac{\varepsilon_t}{kT}\right)_t d\varepsilon . \tag{7.18}$$

That is, the *distribution function* $f(\varepsilon_t)$ of the *relative translational energy* is proportional to

$$f(\varepsilon_t) \propto \varepsilon_t^{3/2-\omega} \exp\left(-\frac{\varepsilon_t}{kT}\right),$$

where ω is the temperature power exponent of the viscosity of the (mono-component) gas.

Suppose for different components 1, 2 a temperature power exponent $\omega_{1,2}$ of viscosity can be determined, then the distribution function of the translational energy in the collision between molecules of components 1 and 2 of the gas mixture can be written as

$$f(\varepsilon_t) \propto \varepsilon_t^{3/2-\omega_{12}} \exp\left(-\frac{\varepsilon_t}{kT}\right). \tag{7.19}$$

The total energy E_c in the collision is the sum of the relative translational energy ε_t and the total internal energy E_i

$$E_c = \varepsilon_t + E_i . \tag{7.20}$$

According to Eqs. (7.16) and (7.19) the distribution function of the translational energy ε_t and the total internal energy E_i can be written as

$$\varepsilon_t^{3/2-\omega_{12}} E_i^{\overline{\zeta}-1} \exp\left[-\frac{(\varepsilon_t + E_i)}{kT}\right],$$

or

$$\varepsilon_t^{3/2-\omega_{12}}\left(E_c-\varepsilon_t\right)^{\overline{\zeta}-1}\exp\left[-\frac{E_c}{kT}\right].$$

As the effective temperature T in the collision is determined by the total energy E_c in the collision (see Eq. (7.26) to appear in the following), so the exponential term is a constant, and the translational energy in the collision is proportional to

$$\varepsilon_t^{3/2-\omega_{12}}\left(E_c-\varepsilon_t\right)^{\overline{\zeta}-1}. \tag{7.21}$$

In the collision the total energy $E_c=\varepsilon_t+E_i=\varepsilon_t+\varepsilon_{i1}+\varepsilon_{i2}$ remains unchanged. In the inelastic collision the translational energy ε_t^* and the internal energy after collision are sampled according to the equilibrium distribution Eq. (7.21), i.e. , ε_t^*/E_c is sampled by the acceptance-rejection method from the following expression

$$f\left(\frac{\varepsilon_t^*}{E_c}\right)\propto\left(\frac{\varepsilon_t^*}{E_c}\right)^{\frac{3}{2}-\omega_{12}}\left(1-\frac{\varepsilon_t^*}{E_c}\right)^{\overline{\zeta}-1}, \tag{7.22}$$

the *relative velocity after collision* is obtained thereby equal to $\sqrt{2\varepsilon_t^*/m_r}$.

From Eq. (7.15) it is seen that the distribution of the post-collision internal energy $E_i^*=E_c-\varepsilon_t^*$ between the two molecules is sampled from the following formula by using the acceptance-rejection method

$$f\left(\frac{\varepsilon_{i,1}^*}{E_i^*}\right)\propto\left(\frac{\varepsilon_{i,1}^*}{E_i^*}\right)^{\frac{\zeta_1}{2}-1}\left(1-\frac{\varepsilon_{i,1}^*}{E_i^*}\right)^{\frac{\zeta_2}{2}-1}. \tag{7.23}$$

The description of the Larsen-Borgnakke model given here is aimed at the collisions between molecules of different components in the gas mixture. There is not any difficulty to apply the above method in the description of collisions between mono-component molecules. For the mono-component gas one has in Eq. (7.22) $\omega_{1,2}=\omega$, $\overline{\zeta}=\zeta$, and in Eq. (7.23) $\zeta_1=\zeta_2=\zeta$.

In the analysis leading to Eqs. (7.22) and (7.23) it was implicitly assumed that the internal energy includes all modes of the internal energies. In fact, the internal

energies of various modes after collision can be distributed one by one successively with the translational energy utilizing the Larsen-Borgnakke method, the result will be the same as if to distribute all the internal energy modes together with the translational energy (and then by using Eq. (7.23) to distribute the internal energy among various modes). This can be verified by computation test: for example, the result of distribution of the total internal energy and the translational energy according to Eq. (7.22) and the later distribution of the rotational energy ($\zeta_r = 2$) and the vibrational energy (ζ_v according to Eq. (1.86)) according to Eq. (7.23) is the same as the result of distribution of the rotational energy and the vibrational energy separately with the translational energy according to Eq. (7.22). In Bird's book there is an analytical proof of this inference (see section 5.5 of [2]).

7.4.3 CASES OF DISTRIBUTIONS WITH SINGULARITIES, GENERAIZED ACCEPTANCE-REJECTION METHOD

When distribute various energies in the collisions according to the equilibrium distribution in the Larsen-Borgnakke model, there are the following cases when in the distributions appear singularities.

1. When distribute the initial vibrational energy according to the temperature of the gas, the equilibrium distribution Eq. (1.94) is used

$$f(\varepsilon_v) = \frac{1}{\Gamma(\zeta_v/2)} \frac{\varepsilon_v^{\frac{\zeta_v}{2}-1}}{(kT)^{\zeta_v/2}} e^{-\varepsilon_v/kT}, \tag{7.24}$$

where the number ζ_v of the vibrational degree of freedom (see Eq. (1.86)) is less than 2

$$\zeta_v = \frac{2\Theta_v/T}{\exp(\Theta_v/T)-1} < 2. \tag{7.25}$$

It is seen that, when $\varepsilon_v \to 0$, singularity appears, as the power exponent of ε_v is less than 0. Then it is impossible to use directly the acceptance-rejection method to sample energy according to Eq. (7.24). Near the singularity by using the method of taking the truncated value can not gain the exact result as well. For example by using the truncated value acceptance-rejection method according to Eq. (7.24) to

distribute the vibrational energy, the average of the sampled values could not reach the accurate correct average value $(\zeta_v/2)kT$ (see Eq. (1.95)).

2. The sampling of the translational energy after the collision is done according to Eq. (7.22), when in the collision pair one molecule is monatomic molecule and only the vibrational mode of the other molecule is considered, one has $\zeta_1 = 0,$. Then $\overline{\zeta} < 1, \zeta_2 < 2$ in the equation (7.22) near $\varepsilon_t = E_c$ appears singularity.

3. When the internal energy E_i^* after collision is distributed between the two molecules (according to Eq. (7.23)), and when one or both of ζ_1 and ζ_2 is less than 2, the singularity appears at $\varepsilon_{i,1} = 0$ and $\varepsilon_{i,1} = E_i$. After the assignment of the internal energy to a molecule, the distribution between different modes is also assigned according to Eq. (7.23), then also appears the case of $\zeta_1 < 2$ or $\zeta_2 < 2$ leading to singularity. The combined consideration of vibrational energy and the rotational energy can make number of the degrees of freedom of the internal energy to be $\zeta_i = \zeta_r + \zeta_v$ to avoid the sampling from the singular distribution. But in the initial distribution of the vibrational energy and the distribution of the internal energy after collision between the vibrational and the rotational modes, due to the fact of $\zeta_v < 2$, the singularity is inevitable. In the equation (7.22) and equation (7.24) the possible singularity is the single point singularity, but in equation (7.23) it is possible to have singularities both at $\varepsilon_{i,1} = 0$ and $\varepsilon_{i,1} = E_i$, i.e., it is a double singular distribution.

We developed *the generalized acceptance-rejection method*, or *the combined cumulative distribution acceptance-rejection method*, and resolved the problem of random sampling from the single or double singular distribution [15, 16]. The explanation and the example of application of the method is given in the Appendix III.3.

In handling the vibrational mode of energy besides the problem of appearance of singularities in the distribution another problem raised is how to determine the *effective temperature in the collision* to be used for giving the vibrational degrees of freedom through Eq. (7.25). The total energy in the collision of component 1 is

$$\varepsilon_t + \varepsilon_{i,1}.$$

The number of degrees of freedom of the relative translational energy in the collision with component 2 is (from comparison of Eq. (7.19) and Eq. (1.94))

$$\zeta_t = 5 - 2\omega_{12}.$$

The number of rotational degrees of freedom is $\zeta_{r,1}$, the number $\zeta_{v,1}$ of vibrational degrees of freedom is given by Eq. (7.25). Thus (compare with Eq. (1.95))

$$\varepsilon_t + \varepsilon_{i,1} = \frac{1}{2}\left(5 - 2\omega_{12} + \zeta_{r,1} + \frac{2\Theta_{v,1}/T_1}{\exp\left(\Theta_{v,1}/T_1\right)}\right)kT_1,$$

from where the effective temperature in a collision of component 1 is obtained

$$T_1 = \frac{\left(\varepsilon_t + \varepsilon_{i,1}\right)/k}{\frac{5}{2} - \omega_{12} + \zeta_{r,1}/2 + \frac{\Theta_{v,1}/T_1}{\exp\left(\Theta_{v,1}/T_1\right) - 1}}. \tag{7.26}$$

This temperature is determined from the method of iteration, after this the number of degrees of freedom of component 1 is determined from Eq. (7.25).

7.4.4 LARSEN-BORGNAKKE METHOD FOR DISCRETE ENERGY LEVELS

In section 1.3 of Chapter 1 we have seen that the continuum distribution Eq. (1.94) (i.e., Eq. (7.24), where ζ_v is given by Eq. (1.86), i.e., Eq. (7.25)) of the vibrational energy is actually derived from the discrete distribution. And as the spacing between the vibrational energy levels is quite large (see section 1.1), it is appropriate to characterize the vibrational energy of the molecules directly by the discrete energy levels. Haas et al. [17] and Bergemann and Boyd [18] expanded the Larsen-Borgnakke method to the discrete energy levels. The implementation of it in the DSMC simulation is direct and simple, and is introduced here.

The harmonic oscillator model of the quantum mechanics gives the vibrational energy of level n (see Eq. (1.16), Eq. (1.77))

$$\varepsilon_{v,n} = nh\nu = nk\Theta_v, \quad n = 0,1,2,\cdots, \tag{7.27}$$

where

$$\Theta_v = h\nu / k .$$

The equilibrium distribution function of the vibrational energy is Eq. (1.68)', where Q_v is given by Eq. (1.79). Substituting the values of Eq. (7.27) and introducing the Dirac δ function, one can write this distribution in the following form

$$f(\varepsilon_{v.n}) = \frac{1}{kT}\left[1-\exp\left(-\frac{\Theta_v}{T}\right)\right]\times \exp\left(-\frac{\varepsilon_v}{kT}\right)\delta(\varepsilon_v - nk\Theta_v) . \tag{7.28}$$

Now consider the redistribution of the energy levels after collision of a molecule of vibrational energy level n. The total energy in the collision in such case is $E = \varepsilon_t + \varepsilon_v = \varepsilon_t + nk\Theta_v$. The distribution of ε_t is given by Eq. (7.19), the distribution function of the combination of ε_t and ε_v is proportional to

$$(E_c - \varepsilon_v)^{3/2-\omega_{12}} \exp(-E_c/kT)\delta(\varepsilon_v - nk\Theta_v) . \tag{7.29}$$

The assignment of the energies after collision follows the distribution

$$(E_c - \varepsilon_v^*)^{3/2-\omega_{12}} \exp(-E_c/kT)\delta(\varepsilon_v^* - n^*k\Theta_v) . \tag{7.30}$$

Because E_c is a constant, so the exponential term is constant. Normalizing the above formula by its maximum value (at $\varepsilon_v = 0$), one obtains the distribution after the collision

$$\left(1-\frac{\varepsilon_v^*}{E_c}\right)^{3/2-\omega_{12}} \delta(\varepsilon_v^* - n^*k\Theta_v) . \tag{7.31}$$

Or write it in a form of discrete value

$$\left(1-\frac{n^*k\Theta_v}{E_c}\right)^{3/2-\omega_{12}} . \tag{7.31)'}$$

To this distribution apply the acceptance-rejection method to determine, whether the energy level n^* after collision is selected or not. n^* is an integer selected from the interval 0 to $n^*_{\max}$ with uniform probability, where

$$n^*_{\max} = \lfloor E_c/(k\Theta_v) \rfloor . \tag{7.32}$$

The symbol $\lfloor \quad \rfloor$ represents rounding-off.

7.4.5 RELAXATION COLLISION NUMBER AND VIBRATIONAL EXCHANGE PROBABILITY

The above discussion concerns inelastic collisions. If in the DSMC simulation all collisions without limitation were implemented as inelastic collisions, the process of change from one state to anther of the internal (vibrational ad rotational) energies would be too fast, i.e. , the rate of change would be different from the rate of the actual physical relaxation process. In general, the relaxation time τ_i is introduced to characterize the rate of change of the state, this is the time needed for the deviation of the state function (temperature) to decay to $1/e$ of the initial deviation when tends to equilibrium. This time is usually several times large than the collision time

$$\tau_i = Z_i/\nu . \tag{7.33}$$

Z_i is called the *relaxation collision number*, e.g., Z_v is the vibrational relaxation collision number, Z_r is the rotational relaxation collision number. There are a number of works investigating the vibrational and rotational relaxation times and relaxation collision numbers [19, 20]. For the general purpose of computation (basing on the comparison with the experimental data) usually adopt $Z_r = 5$ and $Z_v = 50$, and in the DSMC calculation the proportion of the elastic collisions to the inelastic collisions controlled as $(1-1/Z_r - 1/Z_v):(1/Z_r):(1/Z_v)$ can maintain roughly the relaxation rates of rotation and vibration.

One can introduce the exchange probability ϕ_v of the vibrational energy in the collision to characterize the vibrational relaxation process. The average collision probability P_v in each collision can be expressed through the *exchange probability* ϕ_v of the vibrational energy

$$P_v = \frac{1}{\tau_v \nu} = \int_0^\infty \phi_v(E_c) f\left(\frac{E_c}{kT}\right) d\left(\frac{E_c}{kT}\right), \tag{7.34}$$

where ϕ_v is supposed to be dependent on the total energy E_c in the collision, where ν is the collision frequency, f is the equilibrium distribution of the energy in the collision (see Eq. (1.94), Eq. (7.26))

$$f(E_c/kT) = \frac{1}{\Gamma\left(\frac{5}{2} - \omega + \zeta\right)} \left(\frac{E_c}{kT}\right)^{\frac{3}{2}-\omega+\zeta} \exp\left(-\frac{E_c}{kT}\right) \tag{7.35}$$

The vibrational energy exchange probability originally was assumed to be the function of the relative velocity c_r and proportional to $\exp(-c^*/c_r)$ (see references [21, 22]). Boyd [23, 24] followed this thread and developed the energy exchange model between translational and vibrational modes, treating the vibrational energy either as continuum distributed or as a set of discrete vibrational energy levels, and letting τ_v follow the experimental data of Millikan and White [19]. As ϕ_v is assumed to be the function of c_r, then the instantaneous ϕ_v manifests the tendency of preferential transfer from vibrational to translational modes for high relative velocity, leading to the violation of the energy equipartition. Boyd used the method of averaging the instantaneous probabilities for all collisions during one time step in one cell and achieved energy equipartition (see [21, 22]). In reference [16] on citing a series of references we showed that the vibrational translational exchange probability not only depends on c_r, but also on the rotational and vibrational energies in the collision, and on this basis ϕ_v is supposed to be dependent on E_c (see Eq. (7.34)), and have the following form

$$\phi_v(E_c) = \frac{1}{Z_0} E_c^{\beta} \exp\left(-\frac{S^*}{\sqrt{E_c}}\right), \tag{7.36}$$

where Z_0, β, S^* are determined by substituting into Eq. (7.34) and comparison with the experimental data, and τ_v is given by the experimental correlation of the relaxation time given by Millikan and White [19]

$$p\tau = nkT\tau = \exp\left(A/T^{1/3} + B\right). \tag{7.37}$$

For nitrogen and $p = 1atm$, $A = 220, B = -24.8$. Substituting Eq. (7.35), Eq. (7.36) into Eq. (7.34) after some mathematical manipulations (see [16]), the expressions of S_*, β, Z_0 are obtained

$$S^* = 2\sqrt{(A/3)^3 k},$$

$$\beta = 2 + \omega + 0.5\zeta,$$

$$Z_0 = \left[2\sqrt{\frac{2}{3}} \frac{\Gamma\left(\frac{5}{2} - \omega\right)}{\Gamma\left(\frac{5}{2} \cdot \omega + \zeta\right)} \exp B \left(\frac{S^*}{2}\right)^{2+\zeta} / \sqrt{\mu} \right] \sigma_{ref} \times \left[\left(\frac{5}{2} - \omega\right) k T_{ref} \right]^{\omega - 1/2}. \quad (7.38)$$

The vibrational exchange probability in the form of Eq. (7.36) is applied to DSMC simulation of the relaxation process from the initial zero vibrational energy to higher equilibrium translational energy, the relaxation process of the vibrational temperature is the same as the result of the relaxation process given by the τ_v of the Millikan-White correlation. Introduction of Eq. (7.36) in the simulation of the exchange of vibrational and translational energies in the quiescent gas reveals the satisfaction of the energy equipartition principle and that the vibrational energy follows the equilibrium Boltzmann distribution.

7.5 SIMULATION OF CHEMICAL REACTIONS

7.5.1 CHEMICAL REACTION RATE COEFFICIENT

In general bimolecular chemical reaction is expressed by the chemical formula

$$A + B \rightleftharpoons C + D. \quad (7.39)$$

A, B, C, D are different molecular components. In the molecular gas dynamics and in DSMC simulation the chemical reaction rate is most conveniently expressed through the change of number densities of molecules, then the rate equation of Eq. (7.39) can be written

$$-\frac{dn_A}{dt} = k_f(T) n_A n_B - k_r(T) n_C n_D, \tag{7.40}$$

$k_f(T)$ and $k_r(T)$ denote the *direst* and *reverse reaction rate constants*, they are only functions of the temperature. Usually the reaction rate constants can be expressed in the following form

$$k(T) = aT^b \exp(-E_a / kT). \tag{7.41}$$

This form of dependence on the temperature T in conformity with the multitudinous experimental data was put forward by Kooij [25] in 1892, a,b are constants, E_a is called the *activity energy*: when $b = 0$

$$k(T) = a \exp(-E_a / kT), \tag{7.42}$$

is called the *Arrhenius formula*. For different chemical reactions a,b,E_a in the reaction rate constant expressed in the form Eq. (7.41) are determined by the experimental data. Eq. (7.41) is called *Kooij* or *Arrhenius-Kooij formula*.

7.5.2 PHENOMENOLOGICAL CHEMICAL REACTION MODEL OF BIRD

When a molecule of component A collides with a molecule of component B, chemical reaction happens with a certain probability. Usually the reaction cross section σ_R is introduced, the ratio σ_R / σ_T of it to the total collision cross section σ_T represents the probability with which the elastic collision leads to chemical reaction and is called *sterical factor*. More over, for the occurrence of the reaction, the total energy E_c in the collision, i.e., the sum of the kinetic energy ε_t in the mass center coordinate system and the internal energy must exceed the activation energy E_a. In the previous section we have obtained the equilibrium distribution $f(E_c/kT)$ of the energy in collision (see Eq. (7.35)). Thus, the probability of occurrence of reaction from the collision between A,B is

$$\int_{E_a/kT}^{\infty} \frac{\sigma_R}{\sigma_T} f(E_c/kT)\, d(E_c/kT). \tag{7.43}$$

Bird [26] introduced a phenomenological model of chemical reaction, the idea is to ensure the reaction rate coefficient realized in the simulation by introducing the appropriate σ_R to be in conformity with that given by the experimental data in the form of Eq. (7.41). Bird supposes that the reaction cross section σ_R depends on E_c and E_a and has the form

$$\begin{cases} \sigma_R = 0, \text{ when } E_c < E_a, \\ \sigma_R = \sigma_T C_1 (E_c - E_a)^{C_2} (1 - E_a/E_c)^{\overline{\zeta}+3/2-\omega_{AB}}, \text{ when } E_c > E_a. \end{cases} \tag{7.44}$$

The total number of collisions between molecules A and B in unit time and unit volume is according to Eq. (2.254)

$$N_{cAB} = n_A \nu_{AB}, \tag{7.45}$$

where ν_{AB} is the collision frequency of an A molecule with the B molecules and is given by Eq. (2.265). The probability of occurrence of reaction in these collisions is Eq. (7.43), in which $f(E_c/kT)$ is given by Eq. (7.35). Thereby the rate of the forward reaction is obtained

$$-\frac{dn_A}{dt} = 2\pi^{1/2} \left(d_{ref}\right)_{AB}^2 n_A n_B \left(\frac{2kT_{ref}}{m_r}\right)^{1/2} \times \left(\frac{T}{T_{ref}}\right)^{1-\omega_{AB}} \frac{C_1}{\Gamma\left(\frac{5}{2} - \omega_{AB} + \zeta\right)} \times$$

$$\int_{E_a/kT}^{\infty} (E_c - E_a)^{C_2} (1 - E_a/E_c)^{\overline{\zeta}+\frac{3}{2}-\omega_{AB}} \left(\frac{E_c}{kT}\right)^{\overline{\zeta}+\frac{3}{2}-\omega_{AB}} \times \exp\left(-\frac{E_c}{kT}\right) d\left(\frac{E_c}{kT}\right).$$

The integral can be expressed through the gamma function. By comparison with Eq. (7.40) the forward reaction rate constant can be written as

$$k_f(T) = \frac{2C_1\sigma_{ref}}{\varepsilon\pi^{1/2}} \left(\frac{2kT_{ref}}{m_r}\right)^{1/2} \frac{\Gamma\left(\overline{\zeta} + \frac{5}{2} - \omega_{AB} + C_2\right)}{\Gamma\left(\overline{\zeta} + \frac{5}{2} - \omega_{AB}\right)} \times \frac{k^{C_2} T^{C_2+1-\omega_{AB}}}{T_{ref}^{1-\omega_{AB}}} \exp\left(-\frac{E_a}{kT}\right), \tag{7.46}$$

where ε is the symmetry factor, $\varepsilon = 1$ for different components, and $\varepsilon = 2$ for $A = B$. Comparison of Eq. (7.46) with Eq. (7.41) determines C_1 and C_2 in the definition of σ_R

$$C_1 = \frac{\varepsilon \pi^{1/2} a}{2\sigma_{ref}} \frac{\Gamma\left(\overline{\zeta} + \frac{5}{2} - \omega_{AB}\right)}{\Gamma\left(\overline{\zeta} + b + \frac{3}{2}\right)} \left(\frac{m_r}{2kT_{ref}}\right)^{1/2} \frac{T_{ref}^{1-\omega_{AB}}}{k^{b-1+\omega_{AB}}}, \tag{7.47}$$

$$C_2 = b - 1 + \omega_{AB}.$$

Substitution of these constants into Eq. (7.44) yields the expression of the reaction probability

$$\frac{\sigma_R}{\sigma_T} = \frac{\varepsilon a \pi^{1/2} T_{ref}^b}{2\sigma_{ref} \left(kT_{ref}\right)^{b-1+\omega_{AB}}} \frac{\Gamma\left(\overline{\zeta} + \frac{5}{2} - \omega_{AB}\right)}{\Gamma\left(\overline{\zeta} + b + \frac{3}{2}\right)} \left(\frac{m_r}{2kT_{ref}}\right)^{1/2} \frac{\left(E_c - E_a\right)^{b+\overline{\zeta}+\frac{1}{2}}}{E_c^{\overline{\zeta}+\frac{3}{2}-\omega_{AB}}}. \tag{7.48}$$

When E_c approaches E_a, this probability should be finite, this requires that $b > -1/2 - \overline{\zeta}$. When $b < -1 + \omega_{AB}$, the reaction probability tends to 0 together with $E_c \to \infty$.

This reaction model of Bird is a phenomenological model. Assigning σ_R the form of Eq. (7.44) is mainly for integrating the expression, but is not based on physical considerations. From the above derivation it is seen, that the gas should be in the equilibrium state (the distribution $f(E_c/kT)$ of the form Eq. (7.35) is used), and many times of collisions is needed. However, the practice has shown, for gas in highly nonequilibrium state and with the consideration of only few collisions, this model can provide the correct order of the value of reaction rate. This model received quite wide application in practice.

7.5.3 A STERICALLY DEPENDENT CHEMICAL REACTION MODEL

We put forward a sterically dependent chemical reaction model. It started from a microscopic criterion of occurrence of the dissociation or exchange reaction as the result of the break down of the chemical bond of a diatomic molecule colliding with another particle, and derived the chemical reaction rate constant in the Arrhenius-Kooij form [27]. Fig. 7.3 shows the case of collision of a diatomic molecule CD with another particle A. v_r is the velocity of A relative to CD, θ_1

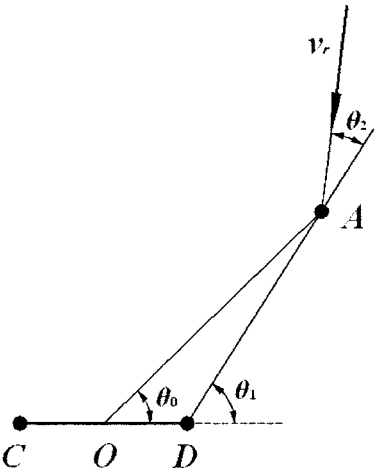

Fig. 7.3 Schematic of collision of a diatomic molecule CD with another particle A

is the angle between CD and DA, θ_2 is the angle between DA and v_r. The microscopic criterion of occurrence of the dissociation or exchange reaction as the result of collision between CD and A is

$$F_w + F_v \geq F_{\max}, \tag{7.49}$$

where F_w is the impact stress occurred in the sphero-cylinder model molecule CD due to collision [28]

$$F_w = \left(k_e m_{CD}\right)^{1/2} v_r \cos\left(\theta_1 + \theta_2\right). \tag{7.50}$$

k_e is the force constant, m_{CD} is the mass of CD. F_v is the stress acting on CD originated from the vibration

$$F_v = \left(2k_e \varepsilon_v\right)^{1/2} \cos\phi, \tag{7.51}$$

ε_v is the vibrational energy, ϕ is the phase angle of CD. $F_{\max}$ is the dynamic breaking factor of the chemical bond CD. Suppose $F_{\max}$ is different from the static breaking factor

$$F_{\max}^{s} = \left(2k_e \varepsilon_D\right)^{1/2}, \tag{7.52}$$

where ε_D is the dissociation energy, but

$$F_{\max} = a_d F_{\max}^{s}, \tag{7.53}$$

where a_d is called the dynamic factor. Substituting Eq. (7.50), Eq. (7.51) and Eq. (7.53) into Eq. (7.49) yields

$$\sqrt{\frac{1}{2} m_{CD}} v_r \cos\left(\theta_1 + \theta_2\right) + \cos\phi \sqrt{\varepsilon_v} \geq a_d \sqrt{\varepsilon_D}. \tag{7.54}$$

The factor a_d is introduced because the configuration of collision may influence the energy structure of the system and change the breaking stress of the chemical bond. This is not contradictory with the fact that the chemical bond energy is a constant. After collision the energy of A and the separated atoms C, D is equal to the total energy of CD and A before collision minus the dissociation energy ε_D. This assumption is in agreement with the theory that in the process of the chemical reaction of two atoms with one collision partner there exists a transitional state [29].

One can suppose that θ_1 and θ_2 are small, for only then the collisions lead to the occurrence of the chemical reaction, so one has

$$\cos(\theta_1 + \theta_2) \approx \cos\theta_1 \cos\theta_2 \approx \cos\theta_0 \cos\theta_2,$$

θ_0 is the angle between OA and CD (O is the middle point of CD), then the equation (7.54) can be written as

$$v_r \cos\theta_0 \geq \frac{a_d \sqrt{\varepsilon_d} - \cos\phi \sqrt{\varepsilon_v}}{\sqrt{\frac{1}{2} m_{CD}} \cos\theta_2}. \tag{7.55}$$

This is the microscopic criterion of occurrence of the chemical reaction. If the factor a_d can be fixed and assume the uniform distribution of ϕ, it is possible to implement the simulation of chemical reaction in the DSMC calculation according to this criterion. But here starting from this criterion we derive the expression of the chemical reaction rate constant

In section 2.11 it is obtained, that the fraction of collision pairs with the kinetic energy, corresponding to the component of the relative velocity along the apse line of the centers of the colliding molecules, exceeding a certain amount of energy ε_0, is $\exp(-\varepsilon_0/kT_t)$ (see Eq. (2.233), for HS model). This is to say, the proportion of collisions in which $v_r\cos\theta_0$ exceeds the right hand side (denoted by v_0) of Eq. (7.55) is $\exp(-m_r v_0^2/2kT_t)$. Basing on this result, integrating over all possible ϕ,θ_2 and ε_v, one obtains the probability of occurrence of the chemical reaction

$$P_r=\frac{2}{\pi^2}\int_0^{\pi/2}\int_0^{\pi}\int_0^{\varepsilon_D}\exp\left[-\frac{m_r}{m_{CD}}\frac{\left(a_d\sqrt{\varepsilon_D}-\cos\phi\sqrt{\varepsilon_v}\right)^2}{\cos^2\theta_2 kT_t}\right]f_{\varepsilon_v}d\varepsilon_v d\phi d\theta_2, \tag{7.56}$$

where f_{ε_v} is the distribution function of the vibrational energy ε_v, which we obtained in Chapter 1 as Eq. (1.94). Thus, we obtained the probability of the chemical reaction

$$P_r=\frac{2}{\pi^2\Gamma(\zeta/2)}\int_0^{\pi/2}\int_0^{\pi/2}\int_0^{t_*}t^{\frac{\zeta}{2}-1}\times\exp\left[-t-\gamma\frac{\left(a_d t_*^{\frac{1}{2}}-\cos\phi t^{\frac{1}{2}}\right)^2}{\cos^2\theta_2}\right]dtd\phi d\theta_2, \tag{7.57}$$

where $t=\varepsilon_v/kT_v$, $t_*=\varepsilon_D/kT_v$, $\gamma=m_A T_v/(m_A+m_{CD})T_t$, ζ is the number of vibrational degrees of freedom, T_v is the vibrational temperature, T_t is the translational temperature. In general case when the temperature is not too high (for N_2 when $T<25000K$), one has $t_*\gg 1$. Then the integral Eq. (7.57) can be calculated approximately. The integral relative to t is (for simplicity, the lower index of θ_2 is eliminated)

$$I=\int_0^{t_*}t^{\frac{\zeta}{2}-1}\exp\left[-t-\gamma\frac{\left(a_d t_*^{\frac{1}{2}}-\cos\phi t^{\frac{1}{2}}\right)^2}{\cos^2\theta}\right]dt. \tag{7.58}$$

This integral can be found by the *method of the steepest descend*. Assume

$$Z = -t - \gamma \frac{\left(a_d t_*^{\frac{1}{2}} - \cos\phi t^{\frac{1}{2}} \right)^2}{\cos^2\theta}. \tag{7.59}$$

It is readily seen that when

$$t = t_m \equiv \frac{a_d^2 t_*}{\left(\frac{1}{\gamma} \frac{\cos^2\theta}{\cos\phi} + \cos\phi \right)^2}, \tag{7.60}$$

one has

$$\frac{dZ}{dt} = 0 .$$

Besides, it is easy to obtain the values of Z_0 and d^2Z/dt^2 at $t = t_m$

$$Z_0 = Z\Big|_{t=t_m} = -\frac{a_d^2 t_*}{\left(\frac{1}{\gamma}\cos^2\theta + \cos^2\phi \right)},$$

$$Z_0 = Z\Big|_{t=t_m} = -\frac{a_d^2 t_*}{\left(\frac{1}{\gamma}\cos^2\theta + \cos^2\phi \right)}.$$

According to the method of the steepest descend one has

$$I = t_m^{\frac{\zeta}{2}-1} \int_0^{t_*} \exp\left[Z_0 + \frac{1}{2}\frac{d^2Z}{dt^2}\Big|_{t=t_m} (Z - Z_0)^2 \right] dt =$$

$$t_m^{\frac{\zeta}{2}-1} \exp\left(-\frac{a_d^2 t_*}{\cos^2\phi + \frac{1}{\gamma}\cos^2\theta} \right) J , \tag{7.61}$$

where

$$J = \int_0^{t_*} e^{-\beta^2 (t - t_m)^2} dt , \tag{7.62}$$

$$\beta = \frac{1}{2}\left[\frac{\cos^2\theta + \gamma\cos^2\phi}{a_d^2 t_* \cos^2\theta}\right]^{1/2}\left(\frac{1}{\gamma}\frac{\cos^2\theta}{\cos\phi} + \cos\phi\right).$$

From the definition of γ and Eq. (7.60) it is seen

$$t_m << t_*,$$

from where one has

$$J \approx \pi^{1/2}/\beta . \tag{7.63}$$

Then the chemical reaction probability Eq. (7.57) can be written

$$P_r = \frac{4}{\pi^{1/2}\Gamma(\zeta/2)}\left(a_d^2\frac{\varepsilon_D}{kT_v}\right)^{\frac{\zeta-1}{2}}\int_0^{\pi/2}\int_0^{\pi/2} \exp\left[-\frac{a_d^2\frac{\varepsilon_D}{kT_v}}{\cos^2\phi + \frac{1}{\gamma}\cos^2\theta}\right]\frac{\cos\theta\left(\gamma\cos\phi\right)^{\zeta-1}}{\left(\gamma\cos^2\phi + \cos^2\theta\right)^{\zeta-\frac{1}{2}}}d\phi d\theta . \tag{7.64}$$

Denote the right hand side integral by M, it can be written by applying the *generalized theorem of mean value* as

$$M = \exp\left[\frac{a_d^2\frac{\varepsilon_D}{kT_v}}{\cos^2\bar{\phi} + \frac{1}{\gamma}\cos^2\bar{\theta}}\right]K(\gamma,\zeta), \tag{7.65}$$

where

$$K(\gamma,\zeta) = \int_0^{\pi/2}\int_0^{\pi/2}\frac{\cos\theta\left(\gamma\cos\phi\right)^{\zeta-1}}{\left(\gamma\cos^2\phi + \cos^2\theta\right)^{\zeta-\frac{1}{2}}}d\phi d\theta . \tag{7.66}$$

The integrals M and K can be evaluated by the numerical quadrature. Define the value of $(\cos^2\phi + \frac{1}{\gamma}\cos^2\theta)$ at some mean value point $(\bar{\phi},\bar{\theta})$ that satisfies Eq. (7.65) as

$$L\left(\gamma,\zeta,a_d^2 t_*\right) \equiv \cos^2\bar{\phi} + \frac{1}{\gamma}\cos^2\bar{\theta}\,, \tag{7.67}$$

and call it the *exponential factor of the reaction rate constant*, then one can write P_r as

$$P_r = \frac{4\left(a_d^2 \dfrac{\varepsilon_D}{kT_v}\right)^{\frac{\zeta-1}{2}}}{\pi^{3/2}\Gamma(\zeta/2)} \exp\left[-\frac{a_d^2}{L\left(\gamma,\zeta,a_d^2 t_*\right)}\frac{\varepsilon_D}{kT_v}\right] K(\zeta,v)\,. \tag{7.68}$$

Note, that when γ,ζ,t_* and a_d are given, K and L are quantities that can be evaluated. Then the reaction rate constant $k_f = \overline{\sigma_T c_r} P_r$ can be written

$$k_f = a T_v^b \exp\left[-\frac{a_d^2}{L\left(\gamma,\zeta,a_d^2 t_*\right)}\frac{\varepsilon_D}{kT_v}\right], \tag{7.69}$$

in which

$$a = \overline{\sigma_T c_r}\frac{4}{\pi^{3/2}\Gamma(\zeta/2)} K(\gamma,\zeta)\left(a_d^2\frac{\varepsilon_d}{k}\right)^{\frac{\zeta-1}{2}},$$

$$b = \frac{1-\zeta}{2}.$$

$K(\gamma,\zeta)$, $L(\gamma,\zeta,a_d^2 t_*)$ are defined by the equation (7.66) and equation (7.67).

The chemical reaction rate constant Eq. (7.69) has the Arrhenius-Kooij form of dependence on the temperature given by the experiments (see Eq. (7.41)), all the parameters appeared in it are determined by the physical properties of the components (CD and A) taking part in the reaction, with the only exception that a_d is determined by comparison of Eq. (7.69) with Eq. (7.41) given by the experimental data. The reaction of the dissociation of nitrogen occurred from its collision with argon

$$N_2 + Ar \rightarrow 2N + Ar\,, \tag{7.70}$$

was provided with the measured data [30, 31] of the reaction rate constant. When in Eq. (7.69) take $a_d = 1.45$ and 1.49, respectively, the rate constants have excellent agreement with the experimental data of [30] and [31].

From both the microscopic criterion Eq. (7.54) and the form Eq. (7.69) of the reaction rate constant k_f derived from it, it can be clearly seen that the dissociation is dependent on the vibration relaxation. The ratio $k_f(T_v, T)/k_f(T, T)$ obtained from the calculation of the present model is in good agreement with the experimental results [32, 33]. For the detailed comparison concerning the above two issues one can refer to [27].

The success of the chemical reaction model described in this subsection is also in the introduction of the exponential factor of the rate constant. This enables the explanation of the fact that the value of T_s in the *exchange reaction rate constant* $k_f = aT^b \exp(-T_s/T)$ obtained experimentally is usually much less than ε_d/k (see [34, 33]). And this fact seems haven't received reasonable explanation before. Consider the following exchange reactions

$$N_2 + O \rightarrow NO + N, \tag{7.71}$$

$$NO + O \rightarrow O_2 + N. \tag{7.72}$$

Under not too high temperature ($T = 1000K \sim 6000K$) the values of $a_d^2 \varepsilon_d/(L \cdot k)$ (see Eq. (7.69)) at $a_d = 1$ are really much less than ε_D/k and are very close to the values of T_s provided by the experiments (see Table 7.1).

Table 7.1 The T_s values in the exchange reaction rate constant provided by the experiments compared with the T_s values calculated from the present model

Reaction	$\frac{\varepsilon_D}{k}$ [34]	$\frac{\varepsilon_D}{k}$ [33]	T_s [34]	T_s [33]	$\frac{\varepsilon_D}{Lk}$ (when $T = 3000K$)
(7.71)	$113000K$	$113200K$	$37500K$	$38370K$	$37800K$
(7.72)	$76500K$	$75500K$	$19700K$	$19450K$	$26000K$

7.6 COMPUTATION OF COMPLICATED FLOW FIELDS

The space vehicles already developed by mankind (the space ships and the space shuttles) and the space vehicles that will be developed – the space shuttles of various countries and various space earth transportation systems – will more and more fly in the transitional regime and utilize the aerodynamic force gained in it to do the maneuver flight. The understanding of the aerodynamic force and heating on the vehicle in the transitional regime becomes more and more important. The experimental means in this regime is not complete, there is not such a high enthalpy facility that could simulate completely the non-equilibrium effects (satisfying the binary scaling low, i.e., the equality of total enthalpy and $\rho L = cons$, see Eq. (0.3)). The numerical simulation of the aerodynamic force and heating becomes very important. Since 90ties of the 20^{th} century the DSMC method has been applied to solve the flow fields of AFE (Aero-assisted Flight Experiment) vehicle, intersected blunt wedges, the plate with incidence, delta wing, sphere, full scale space shuttle and planet vehicles (Viking and Magellan), the satellites, SSTO (single stage to orbit) vehicle and other configurations.

For the demands in exploring the space it is necessary to continuously develop space vehicles of various configurations satisfying various purposes of the investigation, from the point of view of the users it is desirable to have a high efficiency general program that is readily applied to various complicated configurations and capable of providing exact reliable results. Corresponding to such requirements two types of DSMC simulation programs has been developed, one is the program with unstructured body-fitted grid, the other is the program with the Cartesian coordinate grid.

The body-fitted grid program is developed in the direct simulation of the flow fields of AEF vehicle [35] and delta wing [36,37] by Celenligil and Moss et al., the hexahedron cells are used, each cell is further divided into 6 (or 5) tetrahedron subcells. Such cells are readily combined with the triangle cells characterizing the body surface and can ensure the exact representation of the configuration and the implementation of the correct boundary conditions, and the alignment of the cells are in conformity with gradients of the flow field characteristics. The problem is

that the algorithm of tracing the molecules is rather complicated and time consuming.

The performance of the body fitted grid program was improved by Wilmoth et al. [38]. Preprocessing software was directly used to the unstructured, surface and volume grid generation files, the cell face geometrical quantities were pre-computed, and the accuracy in tracking the molecules through the grid was improved. The improved code was used to the computation of the SSTO vehicle.

The work of systematic use of the Cartesian grid code to solve the problem of flow around complicated configurations was started by the position element method of Bird [39]. The flow field was divided into multilevel Cartesian cells, the most fine level was called the position elements the size of which represents the accuracy of the locations of molecules and boundaries, the surface elements allotted from them determined the surface of the body. Although the surface was of stepped form, but as the direction cosines of the surface were stored, the surface appeared with smooth characteristics. This general code of the position element concept had efficiency of the level of the specific code. The agreement of the lift to drag ratio of the space shuttle thus obtained with flight data [6] demonstrated the bright prospective of the DSMC method in prediction of the flow characteristics in the transitional regime. Rault [40] developed the Cartesian grid code with flexible cell self adaptation, which was readily applied to various configurations, such as the triangle wing, space shuttle, wave rider, AEF vehicle, planet vehicle and the high altitude satellite etc. For the simulation of the high density region of the windward side of the hypersonic vehicle, the local body fitted grid was embedded into the Cartesian grid [41], to describe properly the normal gradients near the wall. In reference [38] a Cartesian grid algorithm was developed called DAC (DSMC Analysis Code), in which the local refinement of the grid was allowed to satisfy the requirement of improving the space resolution. Meanwhile, measures had been taken to ensure the approximate equality of the number of molecules in each cell to enhance the efficiency of computation. Two codes had been utilized to solve the hypersonic rarefied gas flow field of the SSTO vehicle, results in excellent agreement had been obtained for surface quantities, flow field quantities and global aerodynamic characteristics (lift drag ratio, the center of pressure, the pitching moment etc.). The Cartesian grid required less preparation work and was

more efficient, in general judging by the computation time per molecule or per time step, the Cartesian grid software was found 2~10 times faster than the body fitted code.

We suggested a new version of the position element algorithm of using DSMC method to calculate the three dimensional flow in transitional flow regime [42, 43]. This is a general code capable to simulate rarefied gas flow around multiple complicated configurations. The configuration of the vehicle was marked not only by the most frontier and the most rear position element cubes, but all the position element cubes that intersect with the body surface were marked as surface elements. Whether the body was presented analytically or by digital data, the points of intersection of the arrises of the surface element cubes with the body surface were exactly determined, and the area ΔS of the body surface (consisted of several triangles) stretched on each surface element was calculated and the directional cosines of its normal were determined and stored. This was a kind of extension of the 2-D scheme 'rectangular subcells with adaptive body fitted cells' [2] to the three dimensions. ΔS was used to calculate the flux characteristics such as heat transfer, pressure and shear, and also to judge on which surface element a molecule is reflected, i.e., the so called probable criterion of collision of molecule with the surface element was used (see [42, 43], the probability of glancing of molecules was taken into account).

In the code the real numbers were used to record the position of molecule, the surface position element was used only to present the form of the body, record ΔS of the surface element and the direction cosines of the normal to the surface, and thereby determine the reflection of the molecules at the surface. Thus, the collision of the moving molecule with the body surface is a deterministic event, the utilization of the above probability criterion of collision could lead to errors. So in [44, 45] a deterministic criterion of collision of molecule with surface element was developed, the reflection of molecule at the surface element was accurately determined.

For either analytical or digital means of presentation of the body configuration, the compiling of the surface element marking program in the position element algorithm of the DSMC is very time consuming. The accomplishment of it by individual user for specific configuration is a very complicated and arduous task.

Reference [45] has made a successful attempt of marking the surface elements by using a general code. This code met some difficulties in treating the nose of the cone, the wingtip of thin aerofoil and other configurations, the apex might be truncated, the tip of the aerofoil might be combined into a single surface. Aiming at such circumstances, in [46] a new method of marking the surface elements is suggested: The body surface is presented by small triangles with apexes located on the plane templates normal to the body axis and equally spaced along the axis of the body; the relations of the surface element-cubes with the body surface triangles are determined; the reflections of the molecules on the surface are accurately tracked by the deterministic criterion of molecular reflection. The position element program embedded with this new surface marking code has been applied to the computation of flows around sphere, the impingement of the 3-D plume onto plate and the force action and the pollution problem of the discharge of residual liquid of a space vehicle of complicated shape [46, 47], showing that the software is convenient and prompt in treating the flow problems of different complicated configurations.

REFERENCES

1. Bird GA (1976) Molecular Gas Dynamics. Clarendon Press, Oxford
2. Bird GA (1994) Molecular Gas Dynamics and Direct Simulation of Gas Flows, Clarendon Press, Oxford
3. Bird GA (1970) Direct Simulation of the Boltzmann equation. Phys. of Fluids, 13: 2676
4. Wagner W (1992) A convergence proof for Bird's direct simulation Monte Carlo method for the Boltzmann equation. J Stat Phys, 66: 1011
5. Pulvirenti M, Wagner W and Zavelani MB (1994) Convergence of particle schemes for the Boltzmann equation. Euro J Mech., B7: 339
6. Bird GA (1990) Application of the DSMC method to the full shuttle geometry. AIAA paper, 90-1692
7. Mott-Smith HM. (1951) The solution of the Boltzmann equation for a shock wave. Phys. Rev., 82:885
8. Pham-Van-Diep G, Erwin D and Muntz EP (1989) Nonequilibrium molecular motion in a hypersonic shock wave. Science, 245: 624
9. Koura K (1986) Null-collision technique in the DSMS method. Phys. of Fluids, 29: 3529
10. Ivanov MS, Rogazinskii SV (1988) Comparative analysis of algorithms of DSMC in rarefied gas dynamics. Comput. Math and Math Phys, 23 (7): 1058

11. Bird GA (1989) Perception of numerical methods in rarefied gas dynamics. Progress in Astro & Aeronautics, 118: 211
12. Fan J, Shen C (1992) A new algorithm in DSMC method –the randomly sampled frequency method. In: The theory, methods and applications of CFD, Science Press, Beijing, p.127 (in Chinese)
13. Larsen PS and Borgnakke C. (1974) Statistical collision model for simulating polyatomic gas with restricted energy exchange. In: M Becker and M. Fiebig edited Rarefied Gas Dynamics, A. 7-1, DFVLR-Press
14. Borgnakke C, Larsen PS (1975) Statistical collision model for Monte Carlo simulation of polyatomic gas mixture. J Comput. Phys, 18: 405
15. Shen C, Wu WQ, Hu ZH, Xu XY (1991) The direct statistical simulation of excitation, relaxation of internal energy and chemical reaction. Acta Aerodynamica Sinica 9: 1-7 (in Chinese)
16. Shen C, Hu ZH, Xu XY and Fan J (1995) Monte Carlo simulation of vibrational energy relaxation in rarefied gas flows. In: J Harvey and G Lord edited Rarefied Gas Dynamics 19, Oxford Univ. Press, 1: 469-475
17. Haas BL, McDonald JD and Dagum L (1993) Models of thermal relaxation mechanics for particle simulation methods. J Comput. Phys, 107: 348
18. Bergemann F and Boyd ID (1995) New-discrete vibrational energy model for the direct simulation Monte Carlo method. Progress in Astro and Aeronautics, 158: 174
19. Millikan RC, White DR (1963) Systematics of vibrational relaxation. J Chem. Phys, 39: 3209
20. Belikov AE, (1989) et al. Preprint 183-88, Institute of Thermophysics, Siber. Branch, Ac Science USSR; Belikov AE, Sukkhinin GI, Sharafutdinov RG (1988) Nitrogen rotational relaxation time measured in free jets. Rarefied Gas Dynamics, Progr. in Astro. And Aeronautics, 117: 40
21. Zener C (1931) Low velocity inelastic collisions. Phys Rev, 38: 277
22. Landau L and Teller E (1936) Theory of sound dispersion. Phys Z Sowjet, 10: 34
23. Boyd ID (1990) Rotational and vibrational nonequilibrium effects in rarefied hypersonic flow. J Thermophysics 4: 478
24. Boyd ID (1991) Analysis of vibrational-translational energy transfer using the DSMC method. Phys. of Fluids, A3: 1785
25. Kooij DM, Z (1893) Phys Chem, 12:155
26. Bird GA (1981) Simulation of multi-dimensional and chemically reacting flows. In: R Campargue edited Rarefied Gas Dynamics, 1: 365, Bird GA (1979) Monte Carlo simulation in an engineering context. Progress in Astro and Aero, 74: Part 1, 239
27. Fan J and Shen C (1995) A sterically dependent chemical reaction model, In: J Harvey and G Lord edited Rarefied Gas Dynamics 19, Oxford Univ. Press, 1: 448
28. Kelsey H (1978) Stress Waves in Solid, Oxford Univ. Press; Miklowitz J (1953) The Theory of Elastic Waves and Wave Guides, North Hollard
29. Laider KJ (1987) Chemical Kinetics (3rd ed), Harper and Row
30. Roth P Thielen K (1986) Measurements of N atom concentrations in dissociation of N_2 by shock waves, Proc. on 15th Shock Waves and Shock Tubes, 245
31. Appleton JP (1968) Shock-tube study of nitrogen dissociation using vacuum ultraviolet light absorption. J Chem. Phys, 48: 599
32. Hansen CF (1991) Dissociation of diatomic gases. J Chem. Phys, 95: 7226
33. Park C (1989) A review of reaction rates in high temperature air. AIAA paper 89-1740
34. Schexnayder CJ Jr and Evans JS (1974) AIAA Jornal,12:805-811

35. Celenligil MC, Moss JN and Blanchard RC (1989) 3-D flow simulation about the AFE vehicle in the transition regime. AIAA paper 89-0245
36. Celenligil MC and Moss JN (1990) Direct Simulation of hypersonic rarefied flow about a delta wing. AIAA paper, 90-0143
37. Celenligil MC and Moss JN (1992) Hypersonic rarefied flow about a delta wing-direct simulation and comparison with experiment. AIAA Journal, 30: 2017
38. Wilmoth RC, LeBeau GJ and Carlson AB (1996) DSMC grid methodologies for computing low-density, hypersonic flow about reusable launch vehicles. AIAA paper 96-1812
39. Bird GA (1990) Application of the DSMC method to the full shuttle geometry. AIAA paper 90-1692
40. Rault DFG (1994) Efficient 3-D DSMC for complex geometry problems. In: BD Shizgal and DP Weaver edited Rarefied Gas dynamics, Progress in Astro & Aeronautics, 159: 137
41. Rault DFG. (1994) Aerodynamics of the shuttle orbiter at high Altitudes. J. of Spacecraft & Rockets, 31: 944
42. Shen C, Fan J, Hu ZH, Wu XY (1996) A new version of position element space discretization in direct statistical simulation of three-dimensional flow in transitional regime. Acta Aerodynamica Siniea 14: 295-303 (in Chinese)
43. Shen C, Fan J, Hu ZH and Xu XY (1997) A new version of position element algorithm of DSMC in calculation of 3-D transitional flows. In: C Shen edited Rarefied Gas Dynamics 20, Peking Univ. Press, 162
44. Fan J, Liu HL, Shen C, Chen LM (2000) A molecular reflection deterministic criterion used in the position element algorithm of direct statistical simulation. Acta Mechanica Sinica 18: 180-187 (in Chinese)
45. Fan J, Peng SL, Liu HL, Shen C, Chen LM (1999) Program marking of surface element and the determination of molecular surface reflection in position element algorithm of DSMC method. Acta Mechanica Sinica 31: 671-676 (in Chinese)
46. Liu HL, Li Z W, Fan J and Shen C Computation of supersonic rarefied gas flows past a sphere .Submitted to Acta Mechanica Sinica (English Series)
47. Fan J, Liu HL, Jiang JZ, Peng SL, Shen C (2004) Analysis and simulation of discharging residual rocket propellants in orbit, Acta Mechanica Sinica 36:129-139 (in Chinese)